A magnetorheological clutch for efficient automotive auxiliary device actuation

F. Bucchi, P. Forte, F. Frendo
University of Pisa – Department of Civil and Industrial Engineering, Largo Lucio Lazzarino, 56122 Pisa (Italy)
francesco.bucchi@for.unipi.it, p.forte@ing.unipi.it, frendo@ing.unipi.it

R. Squarcini
Pierburg Pump Technology Italy S.p.A., Via S.Orlando 12, 57123 Livorno (Italy)
raffaele.squarcini@it.kspg.com

ABSTRACT. In this paper the results of a project funded by Regione Toscana aimed at reducing the power absorption of auxiliary devices in vehicles are presented. In particular the design, testing and application of a magnetorheological clutch (MR) is proposed, aimed at disengaging the vacuum pump, which draws in air from the power-brake booster chamber, in order to reduce the device power absorption.
Several clutch preliminary studies done to choose the clutch geometry and the magnetic field supply are illustrated. The final choice consisted in an MR clutch with permanent magnet, which satisfied size, torque and fail-safe specifications. The clutch characteristics, in terms of torque versus slip, were obtained experimentally for three different clutch prototypes on an *ad-hoc* developed test bench.
As result of a preliminary simulation, a comparison between the power absorption of a current production vacuum pump, an innovative vacuum pump and both vacuum pumps coupled with the MR clutch is presented. The New European Driving Cycle is considered for simulating the vacuum pump operation both in urban and highway driving. Results show that the use of the innovative vacuum pump reduces the device consumption of about 35%, whereas the use of MR clutch coupled with the innovative vacuum pump reduces it up to about 44% in urban driving and 50% in highway driving.

KEYWORDS. Magnetorheological fluid; Magnetorheological clutch; Permanent magnet; Test bench, Experimental testing; Automotive; NEDC.

INTRODUCTION

Nowadays, the reduction of consumption and emissions represents, together with safety and comfort issues, some of the leading trends for vehicle development. Fuel saving is promoted by the increasing attention devoted to environment protection and, at the same time, it is enforced by the pressing regulations on emissions (e.g. current EURO 5 and future EURO 6 emission standards).
The reduction of consumption and emissions is pursued by different strategies, which involve several research fields. The most radical approach deals with the design and implementation of innovative drive-train technologies [1], such as hybrid applications [2] for the short to medium term period, or the use of different fuels [3] (e.g. hydrogen, ammonia, bio-fuels etc.) or different energy supply-chain (pure electric vehicles) for the long term period. However, these solutions often present a long time-to-market and, in some cases, collide with energy processing and storage [2].

Another research field deals with the enhancement of transportation efficiency; current trends aim at reducing the consumptions and emissions by enforcing public transportation or encouraging private vehicles sharing.
At the same time the main OEMs component suppliers and research institutes have been studying several particular solutions aimed at reducing the incidence of auxiliary device absorption (e.g. oil, water and vacuum pumps, air conditioning system etc.), improving the component efficiency (e.g. bearing resistance, seal friction etc.) and reducing the component mass. In particular, the reduction in consumptions is actually analysed with reference to the NEDC driving cycle[4], which takes into account several driving cycles including engine warm-up.
The reduction of oil pump absorptions has been recently studied in [5] by controlling the oil pressure as a function of the engine speed and engine temperature. Other studies [6-7] focus on the control of variable displacement pumps on the basis of the engine oil request. In [8] a switchable water pump was designed in order to disconnect the auxiliary device from the engine when the engine temperature results lower than a threshold value.
Multiphysics research also led to the use of smart materials in vehicle performance optimization. In [9] and [10] the engine cooling fan is driven by a controllable magnetorheological clutch. The use of smart materials permits the regulation of speed and, consequently, of power absorbed by the cooling fan optimizing its operation on the basis of temperature control (e.g. the cooling fan could be disengaged during engine warm-up). The use of smart materials in the automotive industry has been pursued since many years, especially in suspension design [11-13], in order to improve the driver's comfort and the vehicle dynamic performance by changing the apparent viscosity of the MR fluid filling the dampers.
In this paper a multiphysics research aimed at reducing the absorption of vacuum pumps in Diesel engines is presented. The activity was carried out in co-operation between Pierburg Pump Technology (Livorno, Italy) and the University of Pisa, the University of Bologna and the Politecnico of Torino (Italy). Aim of the research, which was funded by Regione Toscana in the framework of the "Bando Unico 2008", was the design of a new vacuum pump, actuated by a magnetorheological clutch.
In particular, this paper describes the development of a fail-safe magnetorheological clutch [14] which was designed for disengaging the vacuum pump from the cam-shaft when its operation is not strictly necessary. The mechanical and magnetic design of the clutch, respectively conceived and developed by the Department of Civil and Industrial Engineering and the Department of Energy, Systems, Territory and Constructions of the University of Pisa, have been proposed and discussed in [15-16]. In this paper, the experimental characteristics of the clutch in the different operating conditions, which were measured on an purposely designed test bench [17], are discussed in comparison with the absorption data of a vacuum pump currently on the market, in order to evaluate the feasibility of a new integrated MR clutch-vacuum pump system.

POWER-BRAKE AND VACUUM PUMP OPERATION

In conventional cars, the braking maneuver is imposed by the driver's pressure on the brake pedal, but the resultant force on the braking master cylinder is amplified exploiting the difference of pressure between two chambers, one connected with ambient air and one (the booster chamber) with the intake manifold, for a throttled gasoline engine, or to the vacuum pump driven by the cam-shaft in Diesel engines [18].
In case of Diesel engines, starting from atmospheric pressure, the vacuum pump draws in air from the booster chamber till the pressure reaches the steady value p_m, as shown in Fig. 1. The emptying time, which is the time taken to reach the pressure steady value p_m, results a function of the cam-shaft speed (it is half the engine speed in 4-stroke engines). In Fig. 1 the emptying trends are shown with reference to a current production vacuum pump (C.P.) and an innovative one (New), which was designed in the framework of the funded project. The engine speed was set at 4000rpm, which corresponds to 2000rpm at the cam-shaft.
If the emptying characteristic is similar for both solutions, significantly different profiles can be found for the absorbed torques, as shown in Fig. 2. The torque profiles were experimentally measured on a vacuum pump test rig. During tests, the oil temperature was imposed at 120°C and the torque was measured at several steady speed values for both the current production and innovative vacuum pump, and the data were interpolated by a piecewise function. During operation, once the saturation pressure p_m is reached in the chamber, the vacuum pump goes on rotating even if its operation is no longer necessary. The power loss could be avoided by disengaging the vacuum pump. The dissipated power can be easily estimated on the basis of the plots of Fig.2, which give the absorbed torque as a function of the cam-shaft speed.

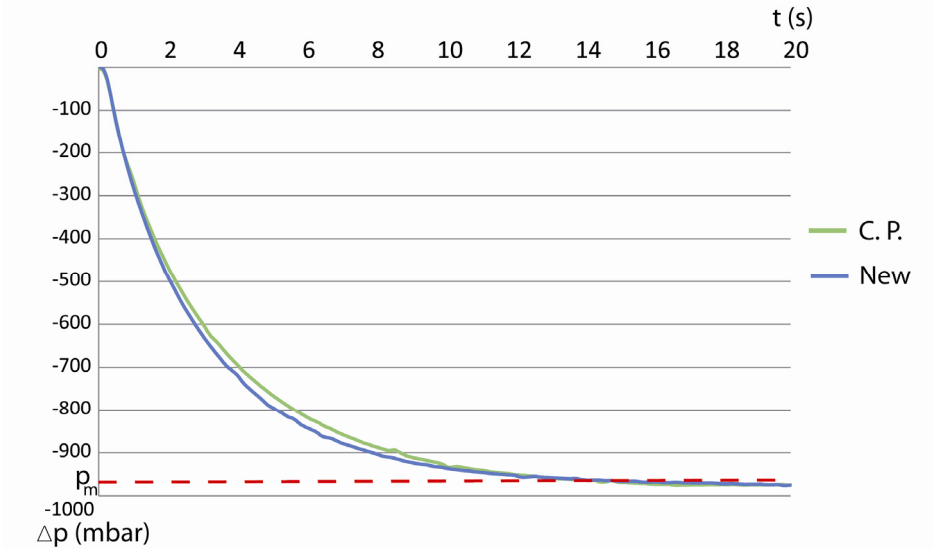

Figure 1: Power-brake booster chamber pressure profile.

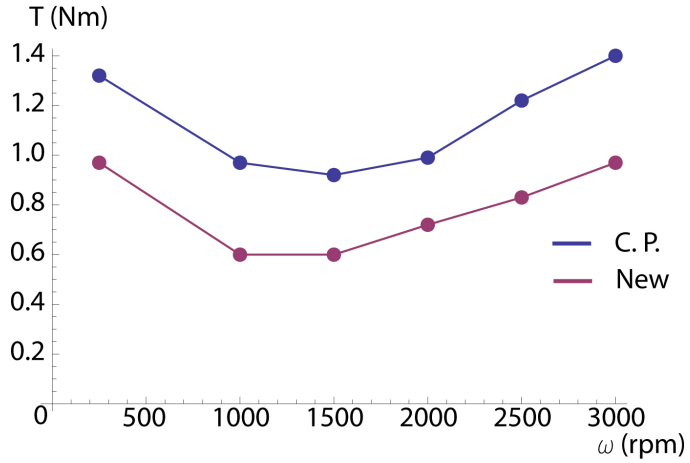

Figure 2: Vacuum pump torque absorption.

VACUUM PUMP DISENGAGING CLUTCH

In order to carry out the disengagement of the vacuum pump, a clutch could be interposed between the cam shaft and the vacuum pump with strict packaging requirements. Due to the pressing safety requests of the braking system, the clutch has to be fail-safe. In addition, no axial load must be exerted on the cam-shaft, so a traditional friction clutch could not be used. The design choice fell on the use of a magnetorheological (MR) fluid clutch, thanks to the peculiar properties of MR fluids listed in the next section.

Magnetorheological fluids

Magnetorheological fluids are suspensions of micro-sized ferrous particles in a carrier fluid [19]. Their main characteristic consists in changing their rheological properties if subjected to a magnetic field. In particular, when not subjected to a magnetic field they behave as Newtonian fluids (N. M.), whereas under the effect of a magnetic field they exhibit a viscoplastic behavior [20], which can be modeled in first approximation by the Bingham-plastic model [21]. According to this model, the stress versus shear-rate characteristic can be considered as the superposition of a rigid perfectly-plastic behavior (characterized by a yield stress value τ_y, which is a function of the magnetic field H) and a linear viscous contribution as shown in Fig. 3.

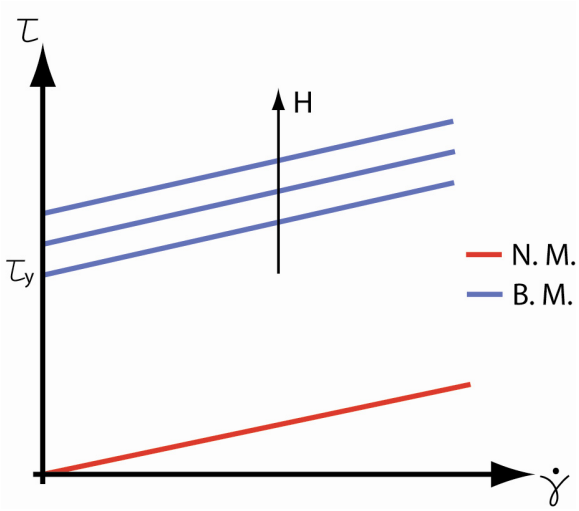

Figure 3: Newton and Bingham models

As regards the vacuum pump disengagement, the following favorable properties of MR fluids have to be considered (numerical values are referred to Lord Corporation MRF140CG fluid):
- low power loss with disengaged clutch due to low viscosity for the unmagnetized fluid (~0.28 Pas);
- high engaged clutch transmissible torque due to high yield stress for the magnetized fluid (~ 55 kPa at 200 kA/m);
- no axial load needed to generate shear stress;
- fast switching time (~10ms) from unmagnetized to magnetized fluid.

Clutch design

On the basis of the design specification listed in Tab. 1, several preliminary design concepts (Fig. 4) were considered in order to define a suitable configuration [15-16]. The comparative analysis of the possible solutions included several FE magnetic simulations which were carried out by the research team of the Department of Energy, Systems, Territory and Constructions of the University of Pisa.

External Diameter	< 70 mm
Overall length	< 50 mm
Engaged torque	> 2.5 Nm
Disengaged torque	< 0.5Nm
Maximum speed	3000rpm

Table 1: Design specifications.

The external diameter and the overall length were limited by the available volume in the proximity of the vacuum pump. The engaged clutch had to assure the torque transmission necessary for the vacuum pump operation, whereas the disengaged clutch torque had to be lower than the torque absorbed by the vacuum pump at steady pressure p_m (Fig. 1). The maximum speed is equal to the maximum envisaged speed of the cam-shaft.
The four basic design given in Fig.4 were taken into consideration. In all solutions with the exception of the first one, the magnetic field is provided by permanent magnets (PM), which assure a fail-safe actuation against possible battery faults.
The analysis of the different geometries allowed to confirm, with the support of quantitative numerical values, that, in order to have a high torque it is necessary to put the MR gap at the larger diameter and, at the same time, to achieve a high magnetic field in the MR gap. Those issues make the solution shown in Fig. 4d, which has a relatively large permanent magnet and an outer MR gap, advantageous with respect to the others; such a solution resulted also conveniently simpler than the multi-disc or multi-cylinder configurations.
A more detailed discussion of the examined geometries can be found in [15].

In addition, in order to compare the capability of the developed prototypes two performance indexes were also proposed in [22]: an exploitation index which is a measure of the magnetic design effectiveness and an efficiency index which is a measure of the overall spurious torque, other than the pure viscous one.
The former is the ratio between the actual (experimentally measured) magnetorheological torque and the maximum ideal magnetorheological torque, which would be available if the entire MR gap was subjected to a uniform magnetic field (the one which takes the MR fluid to saturation).

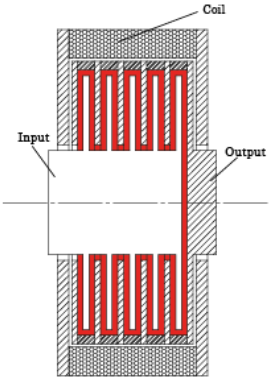

(a) Multidisc with coil.

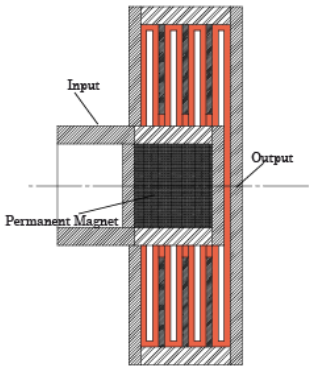

(b) Multidisc with PM.

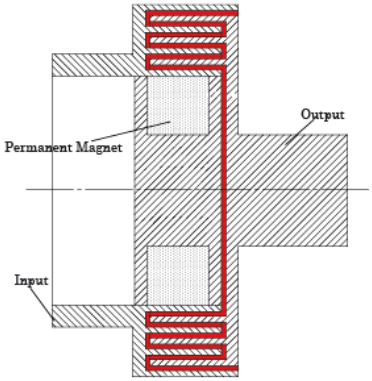

(c) Multicylinder with PM.

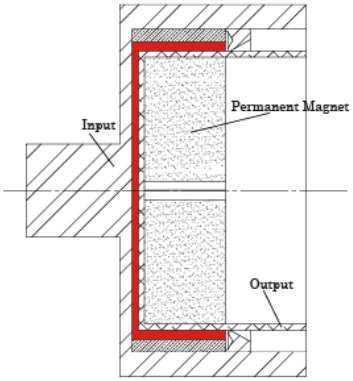

(d) Hybrid (disc-cylinder) geometry with PM.

Figure 4: Preliminary design of the MR clutch

The latter is the ratio between the ideal spurious torque given by the viscous action of the unmagnetized MR fluid and the actual (experimentally measured) spurious torque, which also includes friction in bearings and seals and any possible unwanted magnetization of the fluid for ineffective shielding of the MR gap.
The above indexes are bound in the (0-1) range and can be used to analyze any MR device. In particular, the efficiency index results important in the context of the present research, with respect to the minimization of losses, when the clutch is in the disengaged configuration.

Clutch prototypes

Three prototypes were manufactured on the basis of the layout shown in Fig. 4(d). Each prototype (Fig. 5) consists of an input (primary group) and an output (secondary group) coaxially shafts. The gap between the two groups is filled the MR fluid, which can be magnetized by a rare earth NeFeB PM. The PM can slide in a cylindrical room. When the magnet is positioned close to the fluid (i.e. on the right as in Fig. 5) it assures fluid magnetization and the engaged clutch condition, whereas when it is placed away from the fluid (i.e. on the left, with reference to Fig. 5) its magnetic field is shielded by a ferromagnetic ring fixed to the input shaft and the clutch results disengaged. With regard to the built prototypes, the magnet can be placed manually in the engaged or disengaged mode when the clutch is assembled. A pneumatic actuation system, described hereafter, was developed and will be implemented in future prototypes.

The three prototypes presented the same layout and differed only in the fluid gap external diameter D and length L (Fig. 6). In Tab. 2 the geometrical properties of the clutch are listed together with the torque performance, calculated on the basis of geometrical and fluid data [22] and magnetic finite elements simulations [16].

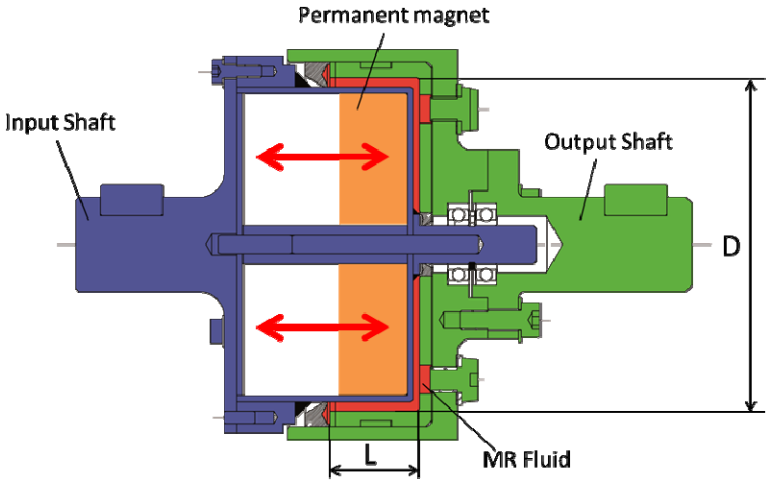

Figure 5: Prototype scheme.

Prototype	D (mm)	L (mm)	T_{ON}(Nm)	T_{OFF}(Nm)
A	57	14	3.1	0.10
B	62	14	3.7	0.17
C	57	19	4.2	0.15

Table 2: Prototype dimensions and torque.

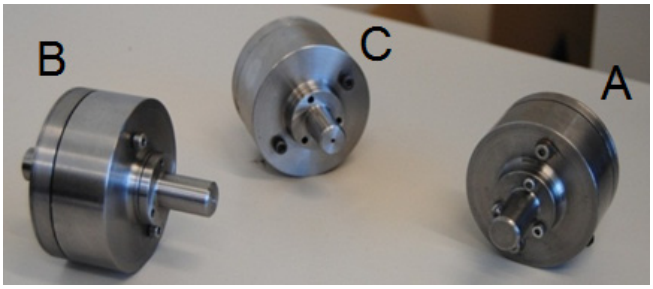

Figure 6: Manufactured prototypes

Clutch actuation

The prototypes shown in Fig. 6 were manufactured in order to validate the numerical model and confirm the expected torque characteristics, and then the magnet movement was not implemented in them. However, the passive automatic actuation schematically shown in Fig. 7 [23] was conceived, in which the left portion of the magnet chamber is directly connected to the vacuum booster and the right chamber communicates with the atmospheric pressure.

A contrast spring forces the magnet to stay close to the fluid until a threshold value for the pressure in the booster is reached and the spring preload is exceeded. From this point the magnet starts moving leftwards, progressively disengaging the clutch. If braking occurs, the pressure in the left chamber rises and the magnet is pushed rightwards by the contrast spring, assuring clutch engagement. In [15] a simplified actuation model is proposed where pneumatic, spring, magnetic and inertial forces are taken into account.

It is evident that the designed system assures the fail-safe operation of the system: if, due to a failure in the pneumatic circuit, the pressure on the left chamber were equal to atmospheric pressure, the clutch would result continuously engaged assuring the continuous actuation of the vacuum pump.

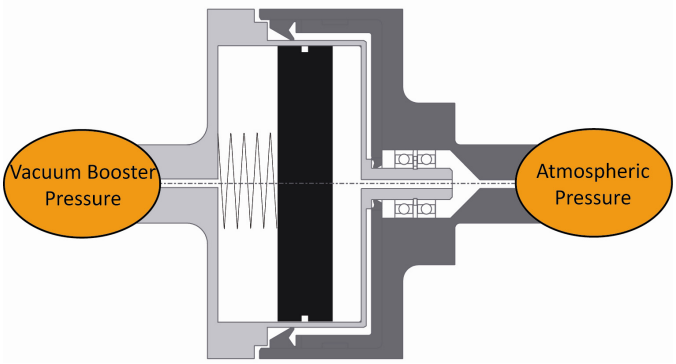

Figure 7: Clutch actuation principle.

EXPERIMENTAL TESTING

Test bench

An experimental test bench was developed in order to characterize the clutch in terms of torque transmitted in engaged and disengaged operating conditions.
Fig. 8 shows the test bench. A brushless motor drives the primary shaft of the rig on which the primary group of the clutch is fastened. The secondary group can be controlled by an asynchronous motor, which imposes the resistant torque or, as shown in Fig. 8, can be kept fixed by means of a plate anchored to the test bench. A torque-meter is mounted on the primary shaft to measure the resistant torque exerted by the secondary group on the primary one, which can be assumed to be equal to the torque transmitted by the clutch. It was verified that the inertial torque due to primary group acceleration can be neglected.

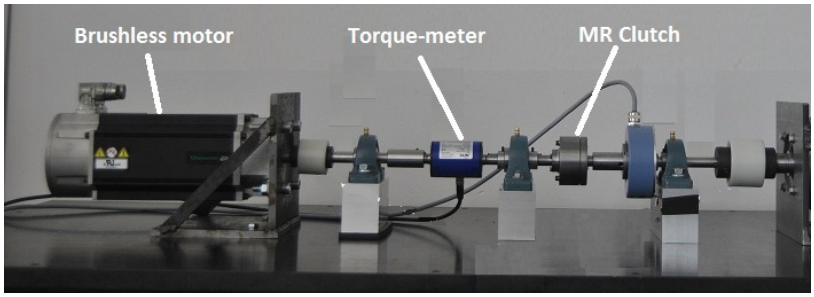

Figure 8: Test bench.

The primary speed is measured by means of a digital encoder embedded in the brushless motor. The rig is also equipped with a digital encoder on the secondary shaft, which could measure the secondary speed if the secondary shaft were not kept fixed.
The testing procedure consists of a constant rate rotational speed profile imposed to the primary shaft which goes from 0 to 1500rpm in about 20s; the test was repeated both with the engaged and disengaged clutch. During the test the torque measured by the torque-meter and the primary speed were acquired.

Torque characteristics of the prototypes

The torque transmitted by the three prototypes is shown in Fig. 9. Subfigures 9(a), 9(b) and 9(c) respectively refer to prototype A, B and C.
As it can be observed the measured characteristic is somewhat different to what envisaged by the Bingham model (see section 3.1). With regard to the torque transmitted by the prototypes in engaged condition it can be pointed out that it results always higher than 2 Nm which, as could be inferred by Fig. 2, is higher than the torque absorbed by both the current production and the innovative vacuum pumps for each operating condition. In particular, prototypes B and especially C present the engaged torque which is considerably higher than 2 Nm. Instead, the maximum torque transmitted by prototype A without any sliding of the groups is close to the maximum torque absorbed by the vacuum pump. If slip occurs, then the torque transmitted by the clutch rises to a greater steady value.

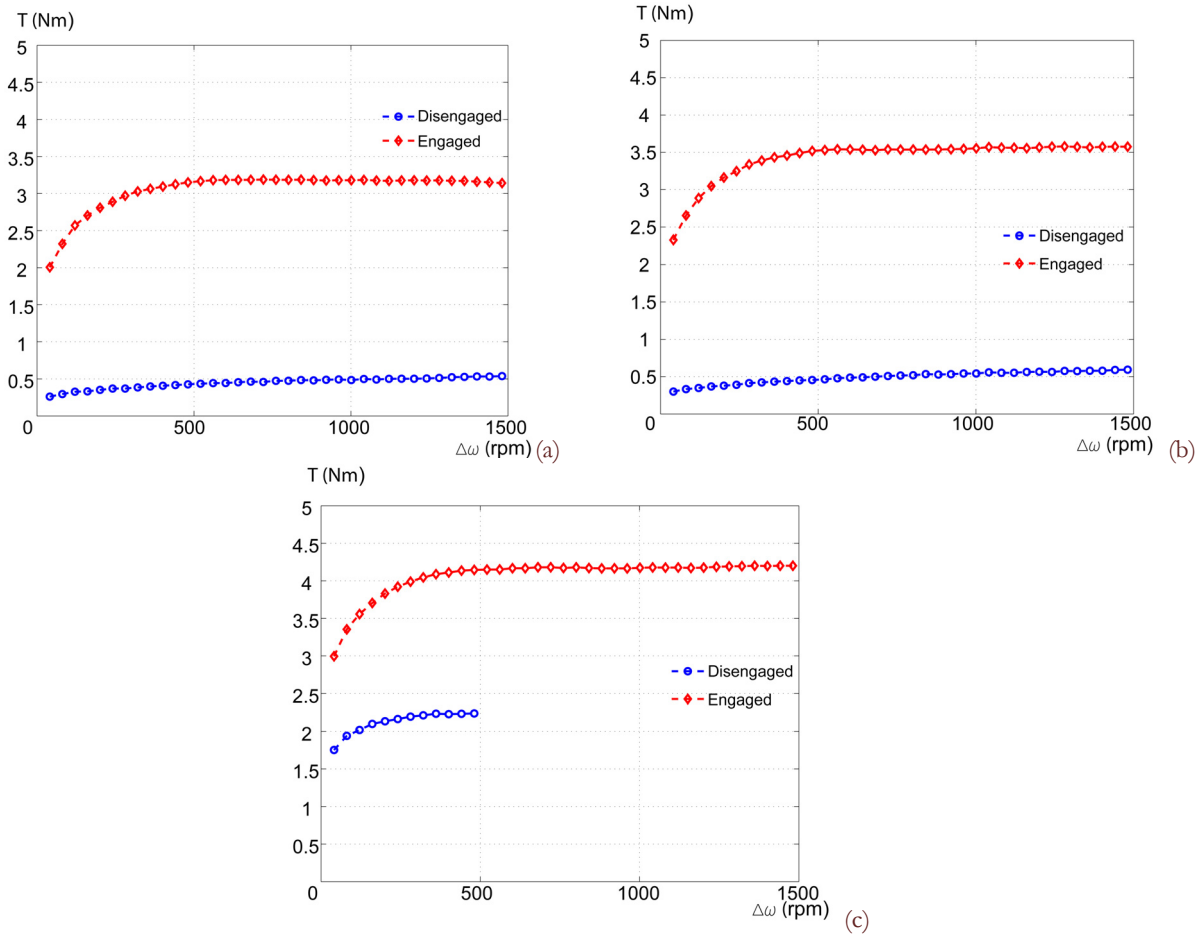

Figure 9: Prototype torque characteristics.

Concerning the torque absorbed by the prototypes in disengaged condition, it is necessary to distinguish between prototypes A and B, which behave correctly, and prototype C, which showed a high value (>1.5 Nm) of the torque absorbed in disengaged mode, due to the partial magnetization of the MR fluid as a consequence of non-efficient shielding of the magnet. In addition, during the test in disengaged condition, some MR leakages occurred and the test could not be performed along the whole range of speed.

On the contrary, prototypes A and B presented a disengaged mode torque which is always lower than 0.6 Nm, that is the minimum value of torque absorbed by the innovative vacuum pump (Fig. 2). For that reason, as shown in Fig. 10, the use of A or B clutch prototype, in disengaged condition, results less wasteful than the vacuum pump rotation.

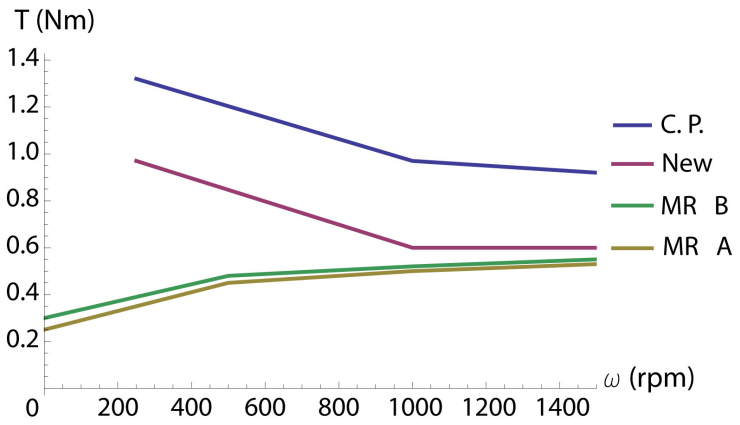

Figure 10: Torque absorbed by current production, innovative vacuum pumps and A and B prototypes.

POWER SAVING

In order to assess the amount of energy saved by the use of the innovative vacuum pump combined with the magnetorheological clutch, a NEDC speed profile was simulated. With regard to the magnetorheological clutch, the torque characteristic considered in the simulations was the one related to prototype A.

The NEDC driving cycle

Vehicle emissions and consumption are usually estimated on the basis of standard mission cycles. In particular, considering mixed missions, one of the most indicated is the NEDC cycle, which is composed by four urban cycles ECE 15, followed by an extra-urban cycle EUDC. For each cycle the profile of speed versus time is proposed, as shown in Fig. 11.

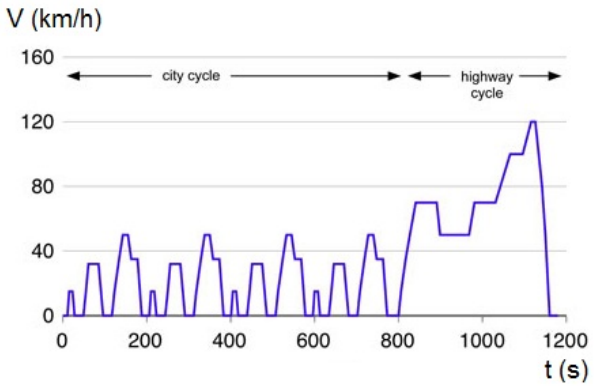

Figure 11: NEDC speed profile.

No information are given about the driver's command to reproduce that cycle, so it is not prescribed any acceleration or braking profile. In order to estimate the pressure in the power-brake vacuum chamber and consequently the need of working of the vacuum pump, it is necessary to assume the breaking use during the cycle. The engine speed profile, as well as the braking use, is not prescribed by the cycle, so the following assumptions were made in order to calculate the power absorption:

- the engine profile was obtained by experimental data made available by an automotive OEM;
- it is considered that every decrease of the engine speed is due to an instantaneous braking maneuver, which causes the complete emptying of the booster chamber.

On the basis of these hypotheses the speed of the camshaft and the need of the vacuum pump can be determined. In particular, the camshaft speed is half the engine speed, whereas the vacuum pump has to be engaged every time a braking occurs and the engagement will last 20s, until the steady pressure p_m in the vacuum pump is reached (Fig .1). Fig. 12 shows the vacuum pump speed profile derived from the previous hypotheses during the NEDC driving cycle.

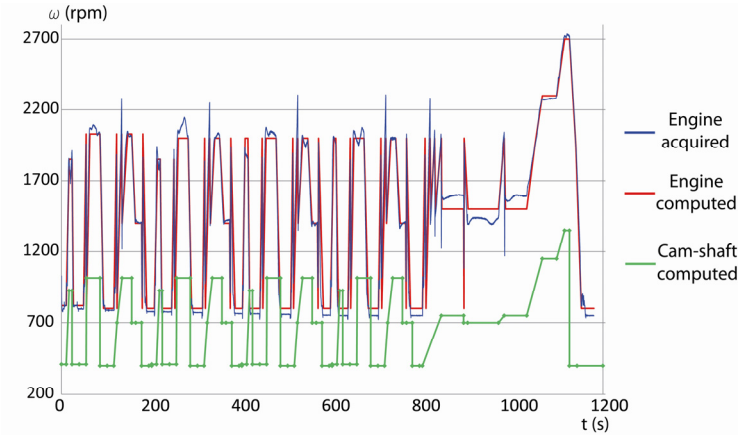

Figure 12: NEDC engine and vacuum pump speed profile.

To identify the need of the vacuum pump the urban and extra-urban cycles were considered separately; then the results were merged considering 4 consecutive urban cycles followed by an extra-urban cycle. Fig. 13 shows the camshaft speed and the need of the vacuum pump during the urban cycle (filled areas indicate the possibility of disengaging the vacuum pump).

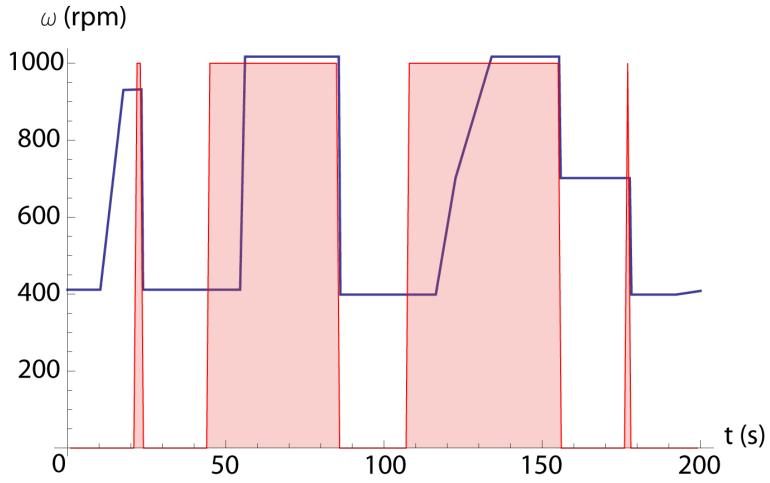

Figure 13: Vacuum pump engagement condition during urban cycle.

In the same way, Fig. 14 shows the need of the vacuum pump during the extra-urban cycle.

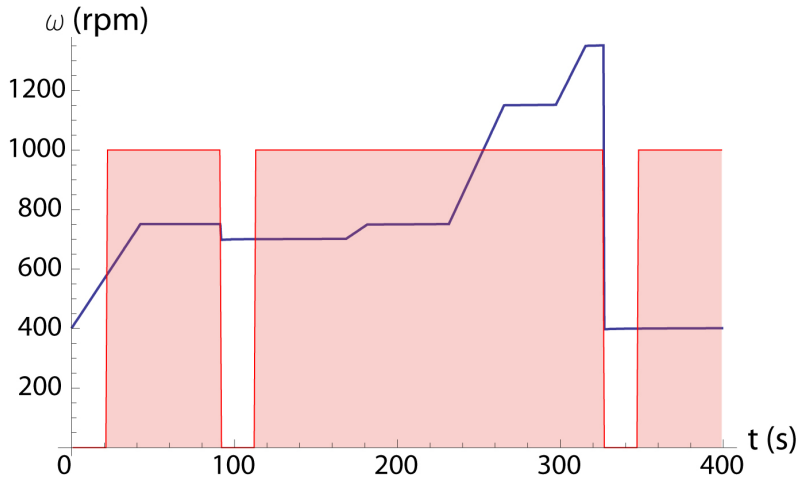

Figure 14: Vacuum pump engagement condition during extra-urban cycle.

Simulation results

The power absorbed by the current production and the innovative vacuum pumps, as well as the power absorbed by the MR clutch prototype, were computed for both urban and extra-urban cycles (Fig. 15) on the basis of the torque characteristics given in Fig. 10 and the vacuum pump speed profile shown in Fig. 12.

Starting from the power curves of Fig.15, the power absorbed by the integrated innovative system, composed of the MR clutch and the innovative vacuum pump, was computed considering the clutch engagement or disengagement previously discussed in Fig 13 and Fig. 14. The power absorbed by the current production vacuum pump is compared to the power absorbed by the innovative system in Fig. 16.

As it can be observed, the latter is switched between the power absorbed by the innovative vacuum pump, when the MR clutch is engaged, or the power absorbed by the MR clutch in the disengaged condition, when the vacuum pump operation is not required.

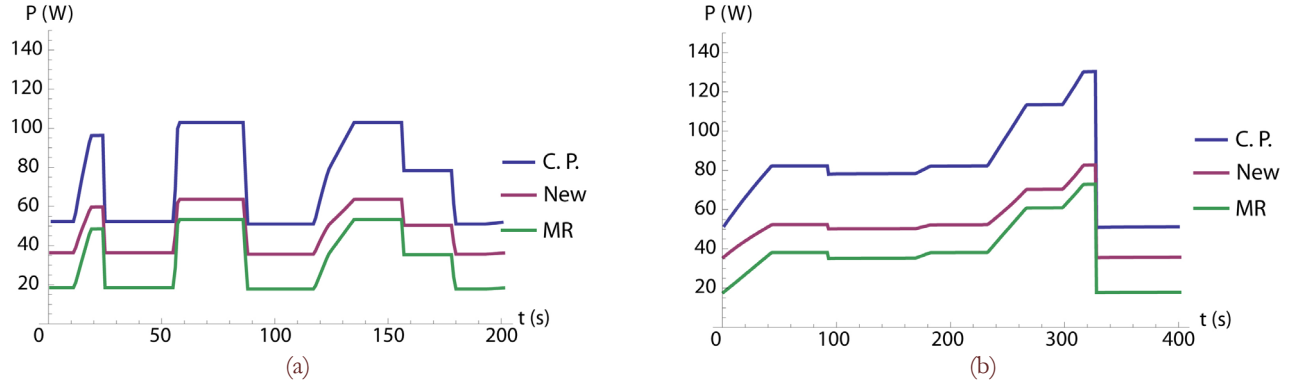

Figure 15: Power absorbed by current production, innovative vacuum pump and MR prototype during urban (a) and extra-urban (b) cycles.

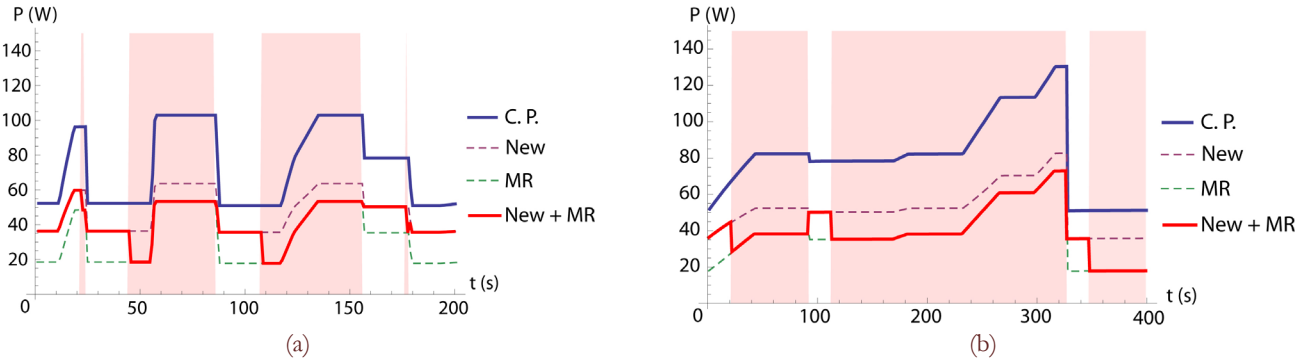

Figure 16: Comparison between power absorbed by current production vacuum pump and integrated clutch-vacuum pump system.

Tab. 3 summarizes the energy absorbed by the following systems, with reference to the elementary cycles taken as reference in the NEDC cycle: current production vacuum pump, innovative vacuum pump, current production vacuum pump coupled with the MR clutch, innovative vacuum pump coupled with the MR clutch.

System	Urban (kJ)	Extra-urban (kJ)	Total (kJ)
Current Production VP	14.6	32.5	90.9
Innovative VP	9.5	20.9	58.9
Current Production VP + MR clutch	10.4	17.5	59.1
Innovative VP + MR clutch	8.2	16.2	49.0

Table 3: Energy absorption during NEDC driving cycle

The energy saved results significant due to both the innovative vacuum pump and to the use of MR clutch. In particular, Tab. 4 shows a comparison between the current production vacuum pump and the aforementioned innovative system.

System	Urban (%)	Extra-urban (%)	Total (%)
Innovative VP	35.0	35.7	35.3
Current Production VP + MR clutch	28.8	46.1	35.1
Innovative VP + MR clutch	43.7	50.3	46.0

Table 4: Energy absorption during NEDC driving cycle.

As expected, the innovative vacuum pump benefits are evident especially during the urban cycle, where the vacuum pump is often engaged, whereas the MR clutch benefits come out especially during the extra-urban cycle when braking maneuvers are infrequent and the vacuum pump can be disengaged for long periods.

CONCLUSIONS

This paper presented the results of a feasibility study regarding an innovative integrated system composed of an MR clutch and the vacuum pump which is used for the power brake system in diesel engines. The innovative system was conceived for reducing the power absorption of the power-brake auxiliaries. In particular, a magnetorheological clutch with permanent magnet aimed at disengaging the engine vacuum pump was designed and three different prototypes were manufactured At the same time an innovative vacuum pump was proposed by Pierburg Pump Technology. The torque transmitted by the three prototypes was obtained from experimental tests both in the engaged and disengaged operating conditions. The experimental campaign allowed to validate the models that were developed in the design stage and also to evidence possible unexpected issues, related to non-perfect shielding and sealing of the MR gap.

A preliminary comparison of the power absorbed by each innovative system (MR clutch and current production or innovative vacuum pump) with that absorbed by the current production vacuum pump was obtained, on the basis of the speed profile prescribed by the NEDC driving cycle, with some simplifying assumptions.

Within the assumed hypotheses, the obtained results showed that the use of the MR clutch contributes to reduce the power absorption with both the current production and the innovative vacuum pump. In particular, the use of the MR clutch coupled with the current production vacuum pump reduces the consumption up to 29% in urban driving and 46% in extra-urban driving. If the MR clutch is used with the innovative vacuum pump the power consumption can be reduced up to 44% in urban driving and up to 50% in extra-urban driving.

ACKNOWLEDGEMENTS

The authors wish to thank Regione Toscana for promoting the research in the framework of the "Bando Unico 2008".

REFERENCES

[1] M. Ehsani, Y. Gao, A. Emadi, Modern Electric, Hybrid Electric and Fuel-Cell Vehicles, CRC Press, (2010).
[2] M. Ceraolo, S. Barsali, G. Lutzemberger, M. Marracci, In: SAE-NA - 9th International Conference on Engines & Vehicles, Capri, Italy (2009).
[3] P. Menga, M. Ceraolo, In: European Ele-Drive Transportation Conference, (2008).
[4] http://www.dieselnet.com/standards/cycles/ece_eudc.php.
[5] M. Rundo, R. Squarcini, In: Proceedings of the ASME 2011 International Mechanical Engineering Congress & Exposition, Denver, Colorado, (2011).
[6] H. Neukirchner, M. Kramer, T. Ohnesorge, SAE Technical Paper, (2002) 1319.
[7] D. Staley, B. Pryor, K. Gilgenbach, SAE Technical Paper, (2007) 1567.
[8] T. Di Giacomo, L. D'Amicantonio, F. Licata, In: Proceedings of Global Powertrain Congress, Munich, 57 (2010) 45.
[9] A. L. Smith, J. C. Ulicny, L. C. Kennedy, J. of Intelligent Material Systems and Structures, 18 (12) (2007) 1131.
[10] E. S. Kim, J. W. Sohn, S. B. Choi, Advanced Materials Research, 79-82 (2009) 79.
[11] G.Z. Yao, F.F. Yap, G. Chen, W. H. Li, S.H. Yeo, Mechatronics, 12 (7) (2002) 963.
[12] M. Ahmadian, C. A. Pare, J. of Intelligent Material Systems and Structures, 11 (8) (2002) 604.
[13] L. D. Ivers, D. LeRoy, In: ASME 2011 Conference on Smart Materials, Adaptive Structures and Intelligent Systems, Scottsdale, Arizona, (2011).
[14] G. Armenio, E. Bartalesi, F. Bucchi, A. Ferri, P. Forte, F. Frendo, R. Rizzo, R. Squarcini, Mechanical combustion engine driven fluid pump, EPO Patent n.114251176.2–2423 (2011.)

[15] F. Bucchi, P. Forte, F. Frendo, A. Musolino, R. Rizzo, A fail-safe magnetorheological clutch excited by permanent magnets. Design and prototype testing, Journal of Smart Materials and Structures, under review.
[16] R. Rizzo, A. Musolino, F. Bucchi, P. Forte, F. Frendo, A fail-safe magnetorheological clutch excited by permanent magnets. Magnetical fem analysis and experimental validation, Journal of Smart Materials and Structures, under review.
[17] F. Bucchi, P. Forte, F. Frendo, In: ESDA Proceedings (ESDA2012-82284), Nantes (2012).
[18] G. Genta, L. Morello, The Automotive Chassis – Vol. 1: Component Design, Springer (2009).
[19] A. Olabi, A. Grunwald, Materials and Design, 28(10) (2007) 2658.
[20] K. Jang, B. Min, J. Seok, J. of Magnetism and Magnetic Materials, 323 (2011) 1324.
[21] E. Bingham, U.S. Bureau of Standards Bulletin, 13 (1916) 309.
[22] F. Bucchi, P. Forte, A. Franceschini, F. Frendo, Investigation on the performance of three differently sized prototypes of a permanent magnet MR clutch for automotive applications, Journal of Mechanical Design, under review.
[23] E. Bartalesi, F. Bucchi, R. Squarcini, Vacuum actuation for axial movement of a magnet in a magnetorheological clutch, EPO European Patent Office, Patent Pending.